J|A|C|S
ARTICLES
Published on Web 03/27/2007

Fluorescent Sensors for Specific RNA: A General Paradigm Using Chemistry and Combinatorial Biology

Brian A. Sparano and Kazunori Koide*

Contribution from the Department of Chemistry, University of Pittsburgh, 219 Parkman Avenue, Pittsburgh, Pennsylvania 15260

Received January 6, 2007; E-mail: koide@pitt.edu

Abstract: Here, we describe a new paradigm for the development of small molecule-based RNA sensors. We prepared a series of potential PET (photoinduced electron transfer) sensors on the basis of 2′,7′-dichlorofluorescein (DCF) fluorophore conjugated with two aniline derivatives as electron donors (quenchers). NMR and fluorescent spectroscopic analyses of these DCF derivatives revealed the correlation between the conformations, the PET, and the fluorescent intensities of these DCF derivatives, enabling us to select a sensor candidate. RNA aptamers were raised against the aniline-based quencher via *in vitro* selection (SELEX). One of these aptamers enhanced the fluorescence intensity of the DCF−aniline conjugate in a concentration-dependent manner. To demonstrate the power and generality of this approach, additional *in vitro* selection was performed and aptamers from this selection were found to have similar activities. These results show that one can develop fluorescence-inducing reporter RNA and morph it into remotely related sequences without prior structural insight into RNA-ligand binding.

Introduction

Fluorescent Imaging of Proteins. The ability to fluorescently label proteins has revolutionized protein imaging and has enhanced our understanding of biology.[1] Proteins are fluorescently labeled through the production of genetically fused chimeras of the target protein with a fluorescent protein such as green fluorescent protein (GFP) (Figure 1B) or through covalent derivatization of specific residues with commercially available organic dyes. Although the GFP approaches can be used to express fluorescently labeled chimeric protein in cells and have found many successful applications, the bulk of GFP can be detrimental to the structure and function of the target protein.[2] Dyes are much smaller than fluorescent proteins, but dye-labeled proteins must be introduced into cells by microinjection. To address both of these problems, Griffin et al. developed the FlAsH method,[3] which allows proteins containing a tetracysteine motif to be expressed and covalently labeled in live cells with a cell-permeable fluorogenic reagent. With this method, it is now possible to rationally design a modular short peptide that can enhance fluorescence when bound to a fluorogenic small molecule.

Fluorescent Imaging of Gene Expression. As described above, conjugation of a target protein with a fluorescent or fluorescence-inducing probe is a powerful method to study the biology of proteins (Figure 1B). Equally important is how each gene expresses the corresponding protein. Since the noncoding regulatory domain of a gene is independent of the gene itself,

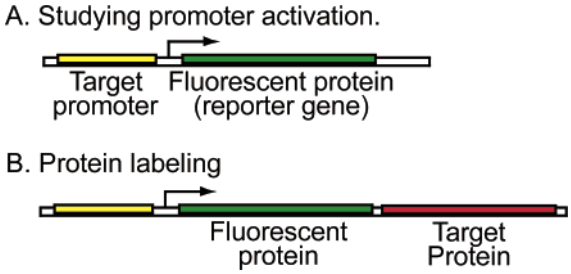

Figure 1. (A) A gene encoding a fluorescent protein is inserted downstream of the target promoter to study promoter's activity. (B) A gene encoding a fluorescent protein is conjugated upstream (shown) or downstream (not shown) of that encoding a target protein to study target protein's behavior.

a commonly used technique to monitor gene expression involves replacing the coding region of the gene with a reporter gene (e.g., GFP,[4] luciferase, β-galactosidase Figure 1A). Expression of the gene results in production of the reporter gene product that then can be measured (fluorescent proteins in the case of GFP or conversion of fluorogenic substrates in the case of β-galactosidase assays).

Fluorescent Imaging of RNA. Although such protein-based reporter assays are powerful methods to determine whether or not a gene is expressed, they do not necessarily reflect RNA levels because the production of an RNA and its corresponding protein are nonlinear in most cases.[5,6] Thus, to obtain more accurate information on gene activation, RNA localization, and processing, it is necessary to be able to "see" RNA in living

(1) Chudakov, D. M.; Lukyanov, S.; Lukyanov, K. A. *Trends Biotechnol.* **2005**, *23*, 605−613.
(2) Giepmans, B. N. G.; Adams, S. R.; Ellisman, M. H.; Tsien, R. Y. *Science* **2006**, *312*, 217−224.
(3) Griffin, B. A.; Adams, S. R.; Tsien, R. Y. *Science* **1998**, *281*, 269−272.
(4) Li, X.; Zhao, X.; Fang, Y.; Jiang, X.; Duong, T.; Fan, C.; Huang, C.-C.; Kain, S. R. *J. Biol. Chem.* **1998**, *273*, 34970−34975.
(5) Gygi, S. P.; Rochon, Y.; Franza, B. R.; Aebersold, R. *Mol. Cell. Biol.* **1999**, *19*, 1720−1730.
(6) Raj, A.; Peskin, C. S.; Tranchina, D.; Vargas, D. Y.; Tyagi, S. *PLoS Biol.* **2006**, *4*, e309.

cells. However, despite the development of aforementioned methods to image proteins, that of analogous methods to image RNA has lagged behind.

Current methods of fluorescent RNA imaging rely on the use of labeled oligonucleotides that have fluorophores covalently bound to one or more bases. These probes are widely used in fluorescent in-situ hybridization (FISH) approaches,[7−9] in which the oligonucleotide probes hybridize to target RNA with Watson−Crick base pairing interactions. Although this method has been used for the detection of RNA[7−9] and transcriptional profiling,[10] it is only able to provide snapshots of dynamic processes like RNA localization[11,12] because the very nature of FISH is that the cells must be fixed (killed) to use this technology. Since one cannot differentiate between the bound and free probe (both are equally fluorescent), FISH techniques are also plagued by high background fluorescence.

To attempt to reduce this background fluorescence, molecular beacons have been developed.[13,14] Molecular beacons contain a stem−loop structure with a quencher proximal to the fluorophore so that the fluorescence is quenched when not hybridized to the target, thereby reducing background fluorescence. Upon hybridization, the probe opens and the quencher is no longer proximal to the fluorophore, restoring fluorescence. Molecular beacons have been used for the visualization and localization of RNA in living cells with much success,[15−17] however, these probes have been shown to nonspecifically bind to proteins and RNA[18,19] and are not membrane permeable. Although FISH and molecular beacon techniques involving fluorescently labeled antisense probes have shed light on many biological questions, they are subject to degradation by nucleases and are not generally applicable to long-term imaging, high-throughput screening, or in-vivo studies. The development of such oligonucleotide-based probes requires substantial optimization requiring several new probes to be designed and tested for each target RNA sequence.

A more general approach toward RNA imaging has recently been reported by Bertrand and co-workers, who used GFP-MS2 (RNA binding protein) fusion protein to detect specific RNA in living cells.[20−22] This technique involves appending a reporter sequence containing dozens of MS2 protein binding sites to the RNA of interest. Although this technique has been used to study RNA localization,[20,23−25] RNA dynamics,[21,26,27] and transcriptional profiling,[22,28] it has several disadvantages. Most significantly, the system inherently suffers from a low signal-to-noise ratio caused by the presence of unbound yet fluorescent MS2-GFP protein. To optimize the signal-to-noise ratio, the expression of the GFP-MS2 conjugate must be tightly regulated using constitutive and drug-inducible expression systems, further complicating live cell experiments.[29]

While other approaches toward the imaging of RNA have been described in the literature,[14,29−31] a more broadly applicable approach would involve a short reporter RNA that is used to enhance the fluorescence of a cell-permeable sensor. The use of a fluorogenic compound responsive to the reporter RNA would greatly reduce background fluorescence thereby increasing sensitivity. This reporter RNA sequence could then be appended to an RNA of interest through standard cloning techniques, thus creating an RNA chimera, or could be used to replace the target RNA, functioning as a reporter gene. Once expressed, this RNA would bind to the fluorescent sensor enabling visualization or detection of the RNA of interest, somewhat analogous to the FlAsH method.

Photoinduced Electron Transfer (PET)-Based Sensors. Since small fluorogenic molecules have seen such limited application in the imaging of biomacromolecules, to design such a sensor, we turned to the field of fluorescent metal ion probes for inspiration.[32−39] An ideal probe for metal ions (or RNA) is nonfluorescent when free in solution and is fluorescent only when bound to a specific target molecule. Such an off−on fluorescent sensor can be rationally designed by implementing the photoinduced electron transfer (PET) mechanism to modulate the fluorescence (Figure 2).[40] When a fluorophore is excited with the appropriate wavelength of light, an electron from the highest occupied molecular orbital (HOMO) is promoted to the lowest unoccupied molecular orbital (LUMO). The decay of this electron back to the HOMO is accompanied by the release of energy in the form of a photon of light (Figure 2a). When a quencher is present near a fluorophore and its HOMO energy level is between the HOMO and LUMO energy levels of the fluorophore (Figure 2b), PET occurs from the quencher to the excited fluorophore, forcing the exited electron to decay by nonradiative means, resulting in reduced fluorescence. The

(7) Rodriguez-Inigo, E.; Casqueiro, M.; Navas, S.; Bartolome, J.; Pardo, M.; Carreno, V. *J. Med. Virol.* **2000**, *60*, 269−274.
(8) Knuchel, M. C.; Graf, B.; Schlaepfer, E.; Kuster, H.; Fischer, M.; Weber, R.; Cone, R. W. *J. Histochem. Cytochem.* **2000**, *48*, 285−294.
(9) Namba, T.; Oida, H.; Sugimoto, Y.; Kakizuka, A.; Negishi, M.; Ichikawa, A.; Narumiya, S. *J. Biol. Chem.* **1994**, *269*, 9986−9992.
(10) Ekong, R.; Wolfe, J. *Curr. Opin. Biotechnol.* **1998**, *9*, 19−24.
(11) Dirks, R.; Daniel, K.; Raap, A. *J. Cell Sci.* **1995**, *108*, 2565−2572.
(12) Kohler, S. *Exp. Parasitol.* **1999**, *92*, 249−262.
(13) Tyagi, S.; Kramer, F. R. *Nat. Biotechnol.* **1996**, *14*, 303−308.
(14) Tan, W.; Wang, K.; Drake, T. J. *Curr. Opin. Chem. Biol.* **2004**, *8*, 547−553.
(15) Bratu, D. P.; Cha, B.-J.; Mhlanga, M. M.; Kramer, F. R.; Tyagi, S. *Proc. Natl. Acad. Sci. U.S.A.* **2003**, *100*, 13308−13313.
(16) Santangelo, P. J.; Nitin, N.; Bao, G. *J. Biomed. Opt.* **2005**, *10*, 044025.
(17) Vargas, D. Y.; Raj, A.; Marras, S. A. E.; Kramer, F. R.; Tyagi, S. *Proc. Natl. Acad. Sci. U.S.A.* **2005**, *102*, 17008−17013.
(18) Browne, K. A. *J. Am. Chem. Soc* **2005**, *127*, 1989−1994.
(19) Dirks, R. W.; Molenaar, C.; Tanke, H. J. *Methods* **2003**, *29*, 51−57.
(20) Bertrand, E.; Chartrand, P.; Schaefer, M.; Shenoy, S. M.; Singer, R. H.; Long, R. M. *Mol. Cell* **1998**, *2*, 437−445.
(21) Fusco, D.; Accornero, N.; Lavoie, B.; Shenoy, S. M.; Blanchard, J. M.; Singer, R. H.; Bertrand, E. *Curr. Biol.* **2003**, *13*, 161−167.
(22) Le, T. T.; Harlepp, S.; Guet, C. C.; Dittmar, K.; Emonet, T.; Pan, T.; Cluzel, P. *Proc. Natl. Acad. Sci. U.S.A.* **2005**, *102*, 9160−9164.
(23) Beach, D. L.; Salmon, E. D.; Bloom, K. *Curr. Biol.* **1999**, *9*, 569−578.
(24) Kloc, M.; Zearfoss, N. R.; Etkin, L. D. *Cell* **2002**, *108*, 533−44.
(25) Singer, R. H. *Curr. Biol.* **2003**, *13*, R673−R675.
(26) Forrest, K. M.; Gavis, E. R. *Curr. Biol* **2003**, *13*, 1159−1168.
(27) Shav-Tal, Y.; Darzacq, X.; Shenoy, S. M.; Fusco, D.; Janicki, S. M.; Spector, D. L.; Singer, R. H. *Science* **2004**, *304*, 1797−1800.
(28) Janicki, S. M.; Tsukamoto, T.; Salghetti, S. E.; Tansey, W. P.; Sachidanandam, R.; Prasanth, K. V.; Ried, T.; Shav-Tal, Y.; Bertrand, E.; Singer, R. H. *Cell* **2004**, *116*, 683−698.
(29) Golding, I.; Paulsson, J.; Zawilski, S. M.; Cox, E. C. *Cell* **2005**, *123*, 1025−1036.
(30) Abe, H.; Kool, E. T. *Proc. Natl. Acad. Sci. U.S.A.* **2006**, *103*, 263−268.
(31) Sando, S.; Kool, E. T. *J. Am. Chem. Soc.* **2002**, *124*, 9686−9687.
(32) Tanaka, K.; Miura, T.; Umezawa, N.; Urano, Y.; Kikuchi, K.; Higuchi, T.; Nagano, T. *J. Am. Chem. Soc.* **2001**, *123*, 2530−2536.
(33) Onoda, M.; Uchiyama, S.; Santa, T.; Imai, K. *Anal. Chem.* **2002**, *74*, 4089−4096.
(34) Hirano, T.; Kikuchi, K.; Urano, Y.; Nagano, T. *J. Am. Chem. Soc.* **2002**, *124*, 6555−6562.
(35) Shults, M. D.; Pearce, D. A.; Imperiali, B. *J. Am. Chem. Soc.* **2003**, *125*, 10591−10597.
(36) Pearce, D. A.; Jotterand, N.; Carrico, I. S.; Imperiali, B. *J. Am. Chem. Soc.* **2001**, *123*, 5160−5161.
(37) Walkup, G. K.; Burdette, S. C.; Lippard, S. J.; Tsien, R. Y. *J. Am. Chem. Soc.* **2000**, *122*, 5644−5645.
(38) Zeng, L.; Miller, E. W.; Pralle, A.; Isacoff, E. Y.; Chang, C. J. *J. Am. Chem. Soc.* **2006**, *128*, 10−11.
(39) Farruggia, G.; Iotti, S.; Prodi, L.; Montalti, M.; Zaccheroni, N.; Savage, P. B.; Trapani, V.; Sale, P.; Wolf, F. I. *J. Am. Chem. Soc.* **2006**, *128*, 344−350.
(40) Lakowicz, J. R. *Principles of fluorescence spectroscopy*, 2nd ed.; Kluwer Academic/Plenum Publishers: New York, 1999.

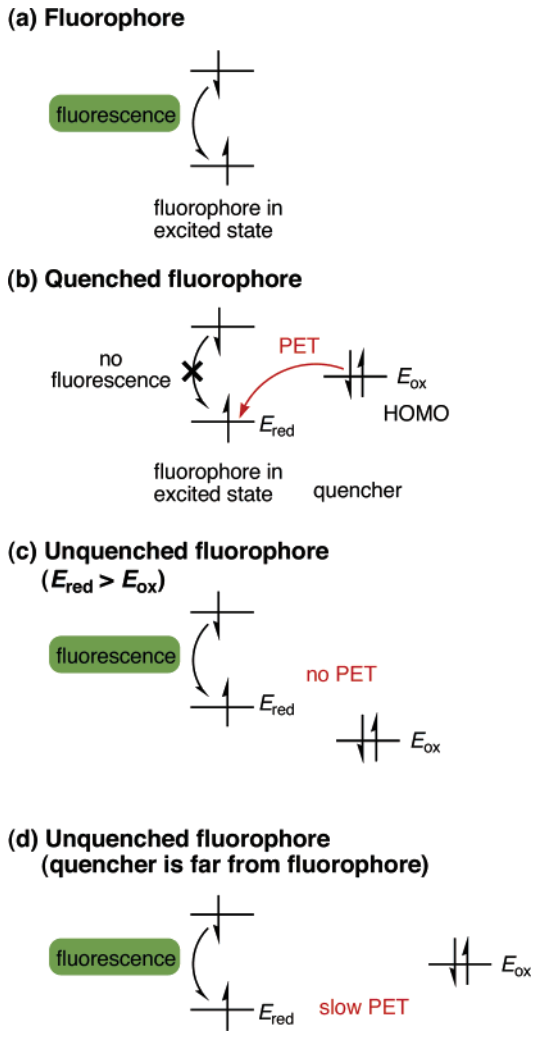

Figure 2. Photoinduced electron transfer (PET)-based switching.

fluorescent intensity of such a sensor is correlated to the HOMO energy level of the quenchers as shown in the Rehm−Weller equation (eq 1; E_{ox} = oxidation potential of a quencher, E_{red} = reduction potential of a fluorophore, ΔE_{00} = the singlet excited energy, w_p = the work term for the charge separation state).[41] As this equation indicates, increasing the HOMO level of the quencher (E_{ox}) thermodynamically favors PET, thus reducing fluorescence signal. The binding of an analyte such as a metal ion can deactivate the quencher by lowering the HOMO level of the quencher, restoring fluorescence (Figure 2c). The correlation between the thermodynamics of the PET process and fluorescent intensity is well established.[42] Ueno et al. described a novel principle for controlling the fluorescence properties on the basis of PET from the singly occupied molecular orbital (SUMO) of an excited fluorophore to the LUMO of a quencher (not shown).[43]

$$\Delta G_{PET} = E_{ox} - E_{red} - \Delta E_{00} - w_p \qquad (1)$$

In principle, the deactivation of the quencher can also be accomplished by increasing the quencher−fluorophore distance,

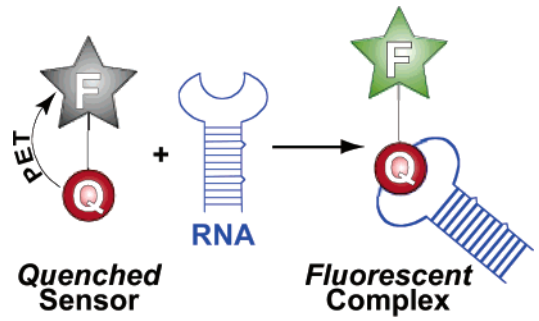

Figure 3. A new approach for RNA sensors.

reducing PET efficiency (Figure 2d). The dependence of quenching efficiency on distance is known to be proportional to $e^{-\beta d}$, where d = the distance between the HOMO electrons of the quencher and the fluorophore. In other words, PET efficiency decreases as the quencher−fluorophore distance increases, allowing efficient radiative decay (i.e., stronger fluorescence) to occur from the LUMO to the HOMO of the fluorophore when the quencher is sufficiently distant. The use of this kinetic switch is rare in sensor development, limited to only a few examples.[44,45]

To summarize PET-dependent fluorescence, for a PET sensor to be switched on, an analyte must lower the HOMO energy level of the quencher or increase the distance between the quencher and the fluorophore.

Results

Design of PET-Based RNA Sensors. In the work presented in this full account,[46] the PET process described above is central to the design of modular fluorogenic sensors. We hypothesized that if a specific RNA binds to the quencher of a PET sensor and either lowers the HOMO level of the quencher or moves the quencher farther from the fluorophore (or better yet, both!), then the result would be fluorescence restoration allowing detection of the RNA−PET sensor complex. This RNA−quencher interaction could then be used to rationally design fluorogenic small molecules that detect that specific RNA. The independence of this RNA−quencher interaction from the fluorophore itself is a key to our approach, opening the door to multiplexed sensing systems with various combinations of fluorophores and RNA ligand (quencher) units (Figure 3).

The modular design of these sensors requires two components: a fluorophore and one or more quencher units. As the fluorophore of our RNA PET sensor, we chose 2′,7′-dichlorofluorescein (DCF). A widely used fluorophore in bioimaging, DCF was chosen because its fluorescence is pH-insensitive under physiological conditions unlike fluorescein (the pK_a of the hydroxy group of DCF and fluorescein are 5.2[47] and 6.5,[48] respectively), DCF is brightly fluorescent (Φ = 0.85), and the chloride groups block two of the possible four nucleophilic centers, enabling us to use DCF as a nucleophile without regioselectivity issues.

Correlation of Quencher HOMO Level to Fluorescence Intensity. To maximize sensitivity, it is important that the

(41) Rehm, D.; Weller, A. *Isr. J. Chem.* **1970**, *8*, 259−271.
(42) Munkholm, C.; Parkinson, D.-R.; Walt, D. R. *J. Am. Chem. Soc.* **1990**, *112*, 2608−2612.
(43) Ueno, T.; Urano, Y.; Setsukinai, K.; Takakusa, H.; Kojima, H.; Kikuchi, K.; Ohkubo, K.; Fukuzumi, S.; Nagano, T. *J. Am. Chem. Soc.* **2004**, *126*, 14079−14085.
(44) Torrado, A.; Imperiali, B. *J. Org. Chem.* **1996**, *61*, 8940−8948.
(45) Sparano, B. A.; Shahi, S. P.; Koide, K. *Org. Lett.* **2004**, *6*, 1947−1949.
(46) For the preliminary results of this work, see: Sparano, B. A.; Koide, K. *J. Am. Chem. Soc.* **2005**, *127*, 14954−14955.
(47) McHedlov-Petrossyan, N. O.; Rubtsov, M. I.; Kukatskaya, L. L. *Dyes Pigm.* **1992**, *18*, 179−198.
(48) Martin, M. M.; Lindqvist, L. *J. Lumin.* **1975**, *10*, 381−390.

Scheme 1. Preparation of Quenched DCF Derivatives via Mannich Reactions. (a) One-Step Protocol from DCF and Secondary Amines. (b) Four-Step Protocol from DCF to Prepare **5**

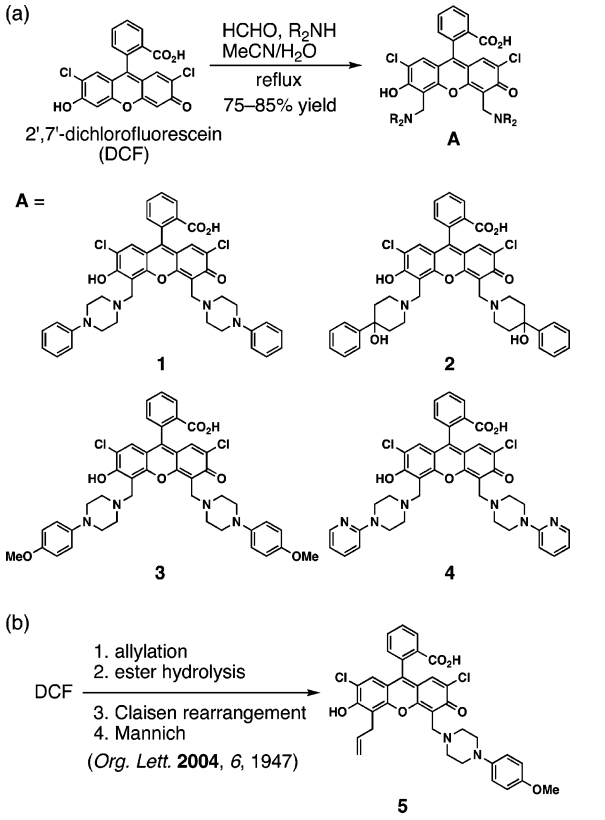

difference in fluorescence from bound to unbound sensor be as large as possible. We needed to find a quencher moiety that would efficiently transfer electrons to the xanthene core of DCF yet be able to have that electron transfer reversibly interrupted by RNA binding. We chose aniline derivatives for this purpose because of their low pK_a values and high HOMO energy levels. To investigate the effect of the aniline nitrogen atoms on the PET mechanism, we coupled DCF to *N*-phenylpiperazine and formaldehyde by means of a Mannich reaction to form compound **1** in 85% isolated yield (Scheme 1a).[45,49,50]

We then gathered spectroscopic data on compound **1** in a pH 7 phosphate buffer (Table 1). As expected, the model compound **1** displayed a low quantum yield (Φ) of 0.052, compared to its parent fluorophore DCF (Φ of 0.85), revealing that compound **1** or its related compounds would exhibit a large increase in fluorescence if the PET can be suppressed. The significant role that the aniline nitrogen atoms played in the PET quenching was confirmed with the lack of aniline nitrogen atoms in compound **2** causing a high Φ of 0.710. This is consistent with the electrons of the aniline system being coupled to the relaxation of the excited chromophore. With this insight, we hypothesized that on the basis of the Rehm−Weller equation (eq 1), the *para*-methoxyaniline derivative **3** would be less fluorescent than aniline derivative **1** because of the higher HOMO level of the aniline system of **3** caused by the electron-donating nature of the methoxy group. This hypothesis was proven when we prepared **3** by the Mannich reaction and found

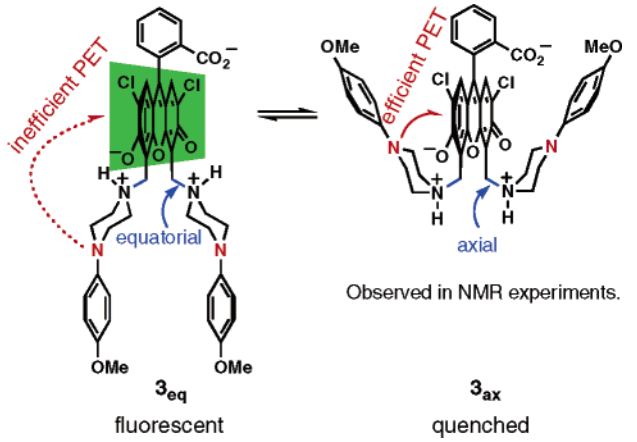

Figure 4. Dynamics of compound **3**.

Table 1. Spectroscopic Data in a pH 7 Phosphate Buffer

compound	λ_{ab-max} (nm)	λ_{em-max} (nm)	Φ
1	507	524	0.052
2	504	522	0.710
3	508	528	0.025
4	508	522	0.102
5	512	533	0.176
DCF	502	522	0.850

the quantum yield of **3** to be 0.025, significantly lower than that of compound **1**.

To further correlate the HOMO energy level of the aniline-based quenchers to fluorescent intensity, we prepared and tested compound **4**. The electron-withdrawing nature of the pyridine ring compared to the phenyl ring should give the quenchers of **4** a lower HOMO level, rendering their quenching less thermodynamically favorable. This is evidenced in the higher quantum yield of compound **4** compared to that of compound **1** (Φ = 0.102 and 0.052, respectively).

To illustrate the effect of the number of quencher units on the fluorescent intensity, we sought to synthesize a monosubstituted analog of compound **3**. However, the Mannich reaction of DCF with 1-(4-methoxyphenyl)piperazine (MPP) generated predominantly the disubstituted compound **3**, even when only 1 equiv of MPP was used. To solve this problem, we developed a synthetic scheme to differentiate between the 4′ and 5′ positions of DCF via the aromatic Claisen rearrangement (Scheme 1b).[45] The quantum yield of **5** was found to be 0.176, suggesting that the quenching of disubstituted compounds **1**−**4** is cooperative rather than additive.

Conformational Analysis. Although we were satisfied by the correlation between the HOMO level of the quencher and the fluorescent intensity, upon closer inspection, the distance between the quenchers and the fluorophore appeared to be too great for efficient PET quenching. As shown in Figure 4 (left), we originally anticipated that compound **3** was in an open conformation where the piperazine rings were in chair conformations with the DCF−methylene unit in the equatorial position. To determine how such seemingly distant aniline nitrogen atoms are able to participate in PET quenching, we investigated the conformation of compounds **1** and **3** on the basis of NOESY

(49) Burdette, S. C.; Walkup, G. K.; Spingler, B.; Tsien, R. Y.; Lippard, S. J. *J. Am. Chem. Soc.* **2001**, *123*, 7831−7841.
(50) Meadow, J. R.; Reid, E. E. *J. Am. Chem. Soc.* **1954**, *76*, 3479−3481.

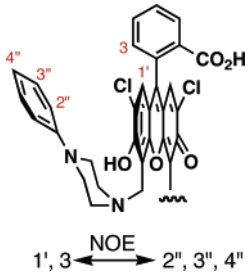

Figure 5. NOESY signals in compound **1**.

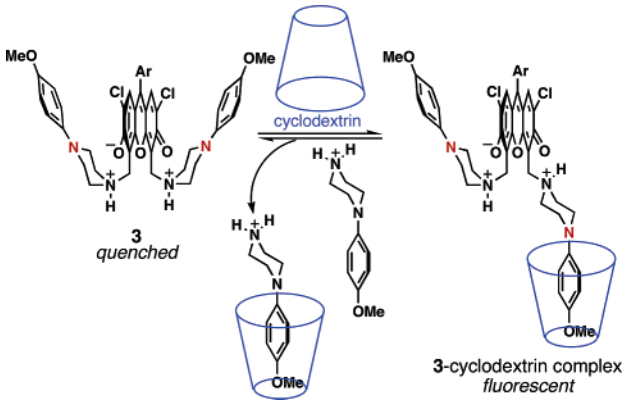

Figure 6. Fluorescence induction of **3** by cyclodextrin.

NMR experiments in DMSO-d_6 (Figure 5).[51] It was immediately apparent from through-space enhancement between the phenyl ring of the quencher moiety and the benzoic acid of the fluorophore that the molecule assumed a closed conformation. This observation means that either the piperazine rings assume a boat conformation (not shown) or the DCF−methylene groups occupy axial instead of equatorial positions. In either case, the aniline nitrogen atoms would be proximal to the xanthene ring of the fluorophore, explaining why the phenylpiperazine moieties are able to effectively quench the fluorescence through space by the PET mechanism. To verify that the sensor candidate **3** shares a similar closed conformation to model compound **1**, a NOESY NMR spectrum was acquired. As predicted, the characteristic NOE enhancements between the quencher and benzoic acid moieties were present.

Correlation of Conformation to Fluorescence. To demonstrate the reversibility of PET quenching in compound **3**, we turned to cyclodextrins (Figure 6). We reasoned that α- and β-cyclodextrin, possessing millimolar affinities for benzene and substituted aromatic systems,[52,53] would bind to the anisole groups of **3**. This would force compound **3** to assume an open conformation, reducing the PET rate as described above and enhancing the fluorescence. Titration of α-cyclodextrin (final concentration 100 mM) into a 5 μM solution of compound **3** yielded a modest 1.7 fold increase in fluorescence. However, with titration of β-cyclodextrin (final concentration 5 mM), we witnessed a 4.6-fold increase in fluorescent intensity.[54] The resulting intensity ($\Phi \sim 0.14$) is similar to that of monosubstituted compound **5** ($\Phi = 0.176$). This correlation, coupled to the steric bulk of β-cyclodextrin, leads us to speculate that β-cyclodextrin and compound **3** form a 1:1 complex in which one of the two *p*-methoxyphenyl groups is bound to β-cyclodextrin. This interaction and resulting conformational change suggests that the unquenching of **3** occurred because the aniline nitrogen atoms of the bound MPP moiety are now too distant from the xanthene ring for efficient PET quenching. To test this hypothesis, we added 1-(4-methoxyphenyl)-piperazine (MPP) to the mixture of **3** and β-cyclodextrin as a competitor for β-cyclodextrin binding. This resulted in a 38% decrease in fluorescence, further supporting our hypothesis.

Scheme 2. Preparation of Affinity Column

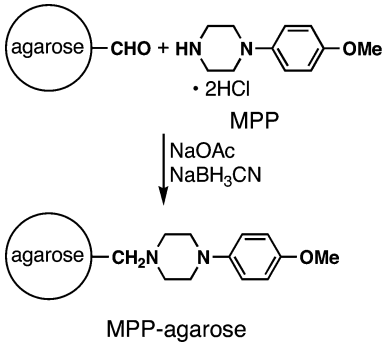

Development of RNA Sensing System. Having established that the fluorescence of our DCF derivatives is modulated by PET quenching (specifically by the HOMO level of the quenchers and the overall conformation of the molecule), we sought to rationally translate this into the development of RNA sensors. Compound **3** is presumably in equilibrium between open (fluorescent) and closed (quenched) conformers (Figure 4). If a specific RNA can be found with the ability to bind only to the open conformer, this interaction will shift the equilibrium toward the fluorescent conformer, resulting in fluorescence enhancement that can be used to visualize the bound RNA. In addition to this conformational change, the RNA may recognize the aniline nitrogen atom of the quencher moiety via hydrogen bonding or chelation, thereby lowering the HOMO energy level of the quencher and potentially resulting in further fluorescence enhancement. The challenge is then to find RNA that only binds to the open conformation despite the fact that compound **3** prefers the closed conformation. In other words, it is crucial to find RNA that does not bind to **3** in such a way as to lock the closed conformation (i.e., weakly fluorescent conformer). Since the binding of cyclodextrins to the MPP moieties of **3** was able to elicit fluorescence enhancement, we reasoned that if RNA that binds to the MPP moieties could be isolated, the resulting conformational change should also elicit a fluorescence increase.

How does one develop RNA that is able to modulate the fluorescence of a PET sensor? We were well aware that it would be a daunting task to rationally design small molecules that both participate in the PET process and bind to specific RNA. Therefore, we chose to rationally design switching into the PET sensors and to look into alternative approaches to rapidly develop ligand-RNA binding systems without the need for prior insight into the specific RNA−small molecule interactions. Since we wished to develop reporter RNAs with universal applicability and minimal interactions with endogenous cellular components (similar to the use of tetracysteine moieties in the

(51) Compound **1** was not sufficiently soluble in D_2O for two-dimensional NMR studies. The quantum yield relationships in DMSO show the same trends as in pH 7 phosphate buffer.
(52) Rekharsky, M. V.; Goldberg, R. N.; Schwarz, F. P.; Tewari, Y. B.; Ross, P. D.; Yamashoji, Y.; Inoue, Y. *J. Am. Chem. Soc.* **1995**, *117*, 8830−8840.
(53) Rekharsky, M. V.; Inoue, Y. *Chem. Rev.* **1998**, *98*, 1875−1918.
(54) The concentration of β-cyclodextrin could not be increased further because of its low solubility.

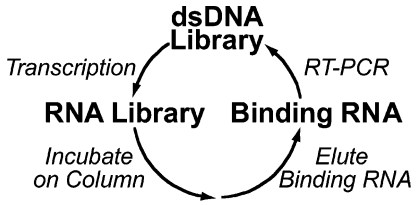

Figure 7. *In vitro* RNA selection.

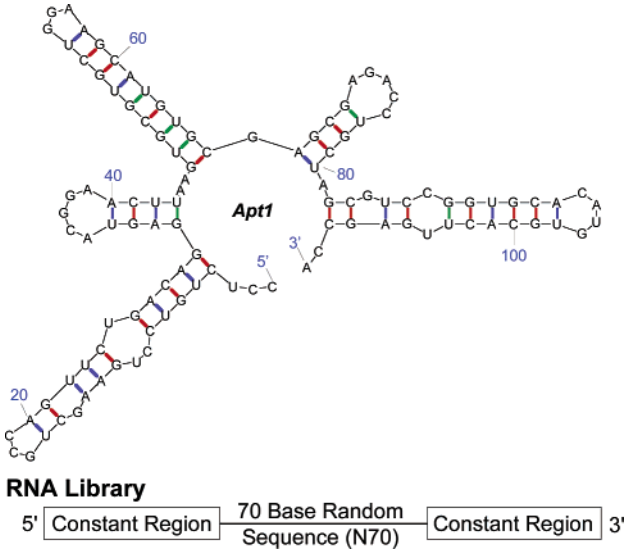

Figure 8.

FlAsH method), we decided to concentrate on the use of artificial RNA sequences. The answer came in the combinatorial biology method *in vitro* selection.

In vitro RNA selection (Figure 7) allows for isolating RNAs that possess a rare activity (RNA aptamers) from a large pool of random RNA (typically 10^{13}−10^{15} molecules).[55−57] To isolate aptamers that bind to a specific ligand, that ligand is typically immobilized on a solid support to be used as an affinity column. The RNA pool is incubated on the column, and the nonbinding RNA is "purified" away. The binding RNA is then eluted and enzymatically amplified to produce a new RNA pool. The process is repeated for several rounds until the pool is dominated by binding RNA.

Isolation of Aptamers for MPP. To isolate aptamers for MPP, we synthesized a random RNA library containing a 70-base random region flanked by 20 base constant regions on the 5′ and 3′ ends for enzymatic manipulation. The layout of the RNA library is depicted in Figure 8 (bottom). Having decided to use MPP as the "bait" on the affinity column to isolate aptamers, we immobilized MPP onto agarose resin (Scheme 2), which was chosen for its ability to swell in aqueous buffers and its demonstrated success.[58−61]

The initial aptamers were isolated in eight rounds of selection from a pool of approximately 10^{13} different RNA sequences. To isolate aptamers that only bind to MPP and not the resin itself, negative selection was employed for the first six rounds,

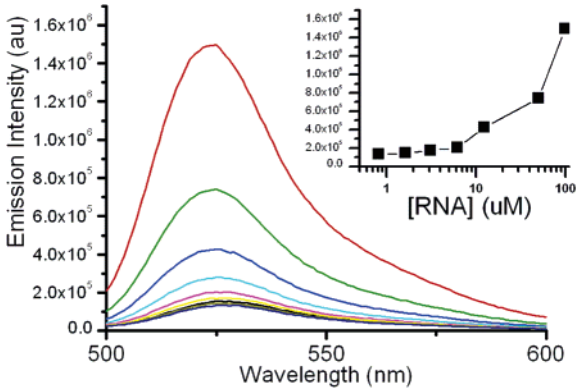

Figure 9. Concentration-dependent fluorescence induction of **3** by **Apt1**.

in which the RNA library was passed over the unsubstituted agarose resin before being incubated with the MPP-agarose resin, thus removing the vast majority of RNA that binds to the agarose portion of the affinity column. To further increase the specificity of the aptamers, after the nonbinding RNA was washed from the affinity column, the binding RNA was then eluted with elution buffer containing 3 mM MPP, preferentially eluting aptamers with affinity for MPP. Once these aptamers were isolated, they were cloned and sequenced. Of the 24 clones sequenced, 18 unique RNA sequences were identified and 3 sequences stood out because of their presence as multiple copies (indicating dominance in the final pool).

These three consensus sequences were then produced on a large scale and were tested for their ability to enhance the fluorescence of **3** by fluorescence titration. The fluorescent intensity of **3** was monitored at RNA concentrations up to 100 μM for each aptamer. Although two of the three aptamers did not demonstrate significant fluorescence enhancement (one showing only 2-fold enhancement and another showing no enhancement), one RNA proved to be different; this aptamer, **Apt1** (Figure 8), was found to enhance the fluorescence of **3** by 13-fold at the 100 μM concentration in a concentration-dependent manner. The lowest energy secondary structure of **Apt1** as predicted by Mfold[62] is depicted in Figure 8. As with the cyclodextrin experiment, the addition of MPP was found to antagonize the fluorescence induction effect, suggesting that **Apt1** binds to the MPP quencher moiety, presumably lowering the HOMO level of the quencher and eliciting a conformational change (moving the quencher away from the xanthene and possibly restricting the rotation of the benzoate moiety) thereby enhancing fluorescence. The titration curve implies that the stoichiometry may be 1:1 (Figure 9). Substituting the random N70 RNA library for **Apt1** did not result in fluorescence enhancement, thus ruling out the possibility of nonspecific interactions between RNA and **3**.

The fluorescence intensity of the **3**-**Apt1** complex exceeds that of compound **5**. If **Apt1** only binds to and deactivates one of the two MPP quencher moieties of **3**, the maximum fluorescence enhancement should be 7-fold (quantum yield: 0.025−0.176). As we were hoping throughout these studies, it is possible that the **3**-**Apt1** binding induces the conformational change of the second MPP because of favorable electrostatic interaction between the positively charged piperazine ring and negatively charged RNA. This conformational change should

(55) Ellington, A. D.; Szostak, J. W. *Nature* **1990**, *346*, 818−822.
(56) Robertson, D. L.; Joyce, G. F. *Nature* **1990**, *344*, 467−468.
(57) Tuerk, C.; Gold, L. *Science* **1990**, *249*, 505−510.
(58) Bartel, D. P.; Szostak, J. W. *Science* **1993**, *261*, 1411−1418.
(59) Holeman, L. A.; Robinson, S. L.; Szostak, J. W.; Wilson, C. *Folding Des.* **1998**, *3*, 423−431.
(60) Sassanfar, M.; Szostak, J. W. *Nature* **1993**, *364*, 550−553.
(61) Wilson, C.; Szostak, J. W. *Nature* **1995**, *374*, 777−782.
(62) Zuker, M. *Nucleic Acids Res.* **2003**, *31*, 3406−3415.

result in an increase in the distance between the second MPP moiety and the fluorophore, leading to further fluorescence enhancement.

Biased Library Selection. We then used the **Apt1** sequence as the basis for a biased library for another selection experiment. A biased library is a library that is partially randomized at each nucleotide position during chemical synthesis. On the basis of literature guidelines,[63] for a library to have ~85% of the molecules with three to eight mutations per molecule, it should have a degeneracy of ~7%. For a library with 7.5% degeneracy, a mixture of 92.5% wild-type base and 2.5% of the other three bases during DNA synthesis would yield a library with ~7.5% of the population having a point mutation at that position.

To increase the stringency of the selection by removing the weak binders, we washed the aptamer-bound column with a 3 μM MPP solution before washing with the 3 mM MPP solution. Again, after eight rounds, the library was cloned and sequenced. Of the 12 unique sequences isolated, three sequences most intrigued us; the first, **AptB1**, was well represented in the library (with five copies in our sampling), the second, **AptB2**, was also well represented with four copies, and the third, **AptB3** (not shown), was the most similar to the wild type, with 87% homology.[64] To test the aptamers for their ability to enhance the fluorescence of compound **3**, the fluorescent intensity was monitored at RNA concentrations up to 50 μM for each aptamer. **AptB3** did not significantly enhance the fluorescence of compound **3**, which is not surprising because of its lack of wide representation in the collection of sequences determined. However, the more represented **AptB1** and **AptB2** aptamers showed 4.1 and 3.8 times enhancement, respectively (their lowest energy calculated secondary structures are shown in Figure 10). This enhancement is comparable to the 4.7 times enhancement exhibited by **Apt1** at 50 μM.

Generality of Combinatorial Biology Approach. To further demonstrate the generality of this approach, we conducted an additional selection using a different random library, identical to the original in the design of the constant regions. This library, although of identical design, is unlikely to contain the same sequences as the original because each 10^{13} random library is only a small fraction of possible sequences in a library containing 70 random bases (1 out of possible 10^{29} sequences). Of the 18 unique sequences isolated by the selection, two sequences were represented by multiple copies in our sampling and thus were tested for fluorescence enhancement. One of these aptamers was shown to enhance the fluorescence of **3** by 4.0 times (**Apt2**, Figure 11). This result is good support for the generality of the approach as we have demonstrated that aptamers capable of fluorescence enhancement can be isolated from each of two completely independent libraries. It is intriguing that **Apt2** has 86% homology to **Apt1**, despite the fact that the two libraries were independently synthesized. Also, the aptamers studied here proved to be quite stable, allowing us to recycle and repurify the RNA many times with no degradation visible by polyacrylamide gel electrophoresis.

(63) Breaker, R. R.; Joyce, G. F. *Trends Biotechnol.* **1994**, *12*, 268−275.
(64) Although not statistically significant, the choice to test only three aptamers was purely an economic one: the expensive process of producing sufficient RNA for evaluating fluorescent enhancement ability restricted us to testing only those aptamers that were well represented in the sequenced hits and lowing the maximum concentration from 100 μM to 50 μM.

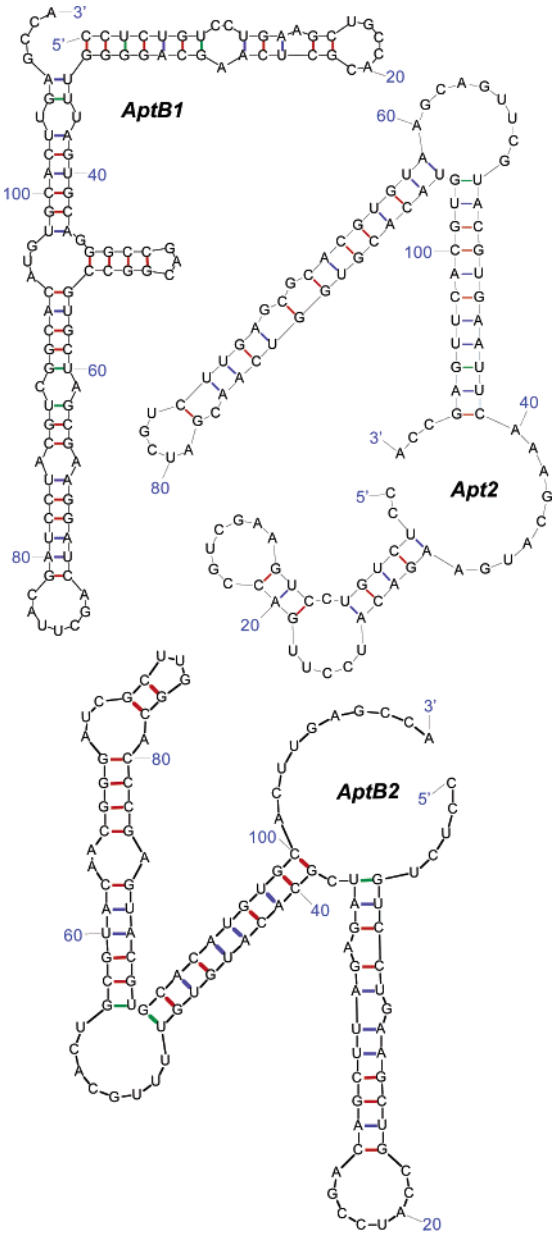

Figure 10. Secondary structures of fluorescence enhancing aptamers.

Discussion

New Paradigm. The new paradigm we present here is a convergence of chemical and biological methods (Figure 12).[65] Through a rational approach toward sensor design, it is possible to synthesize new PET sensors merely by combining existing fluorophores with quenchers possessing appropriate HOMO energy levels, a process that is amenable to building combinatorial chemical libraries of PET sensors. After fluorescent and conformational analysis, candidate sensors are chosen and RNA aptamers are isolated for the quencher units of the selected sensors. Once aptamers have been isolated, the sequence can be morphed into remotely related sequences by further *in vitro* selection. Although we have not presented an example here, the independent nature of the fluorophore and quencher makes it possible to optimize the sensor system by changing the fluorophore to fit the particular experiment. Once a satisfactory

(65) For an account, see: Koide, K. *Am. Biotechnol. Lab.* **2006**, *24*, 8−10.

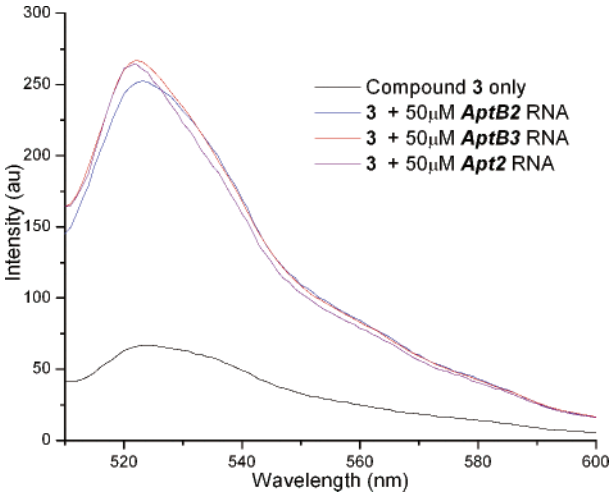

Figure 11.

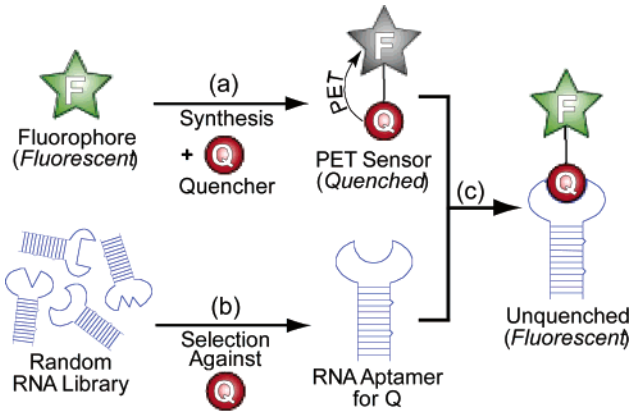

Figure 12. A new paradigm that emerged from this study. (a) Organic synthesis to install quenchers to a fluorophore. (b) *In vitro* RNA selection against the quencher to isolate RNA aptamers against the quencher. (c) Fluorescent spectroscopy to study fluorescent RNA−sensor complexes.

RNA−sensor system is found, the RNA can then be used as a reporter RNA to study gene expression or can be used to tag endogenous RNAs by forming chimeras with the target RNA. Reporter RNA would function in much the same way as the protein reporters discussed above, with the insertion of the artificial RNA sequence downstream of the regulatory domain (similar in concept to Figure 1A). When the gene is activated, the reporter RNA is produced and if the appropriate RNA sensor is present, the RNA will bind to and enhance its fluorescence. In addition to having low background (the sensor is only fluorescent when bound to RNA), such a system will have the advantage of being widely applicable, as the same reporter RNA−RNA chemosensor pair can be used to monitor the expression of virtually any gene. The use of an artificial RNA sequence also has the advantage of being less likely to bind to endogenous proteins. The RNA chemosensor **3**, the aptamers found to enhance its fluorescence, and most importantly the new paradigm they represent are significant milestones toward a small molecule-based RNA expression assay. Our laboratory is currently working toward such an assay through the further optimization of aptamer sequences and the demonstration of this system in living cells.

Improving Sensitivity. Since RNA is scarce in living cells, desirable RNA sensors must be far more sensitive than the system presented here. Although the conformational change of compound **3** is interesting as sensor design, the requirement for RNA to induce a conformational change in compound **3** may be detrimental for developing tighter binding systems because such a binding mode must force the sensor to adopt less favorable conformation. Thus, to develop more sensitive RNA sensors, the following criteria need to be met in the future: (1) the HOMO energy level of a quencher needs to be higher than the aniline derivatives presented here to further suppress the background signal; (2) the quencher should be more complex and chiral to increase binding sites for specific RNA; (3) conformational changes of a sensor upon binding to reporter RNA should be reduced for higher affinity; (4) to achieve objective 3, slightly longer linkers may be needed between a fluorophore and quenchers.

Conclusion

Through the initial isolation of RNA aptamers for quencher units and subsequent demonstration of their ability to enhance the fluorescence of fluorophores derivatized with those quenchers, we have established a new paradigm in the development of biosensors. By isolating additional RNA aptamers that have similar abilities from both libraries on the basis of the original sequence and independent random libraries, we have addressed and shown the generality of this approach.

Experimental Section

General Techniques. Acetonitrile was dried over 3 Å molecular sieves. Yields refer to chromatographically and spectroscopically (^{1}H NMR) homogeneous materials unless otherwise stated. All reactions were monitored by thin-layer chromatography (TLC) carried out on 0.25-mm EMD Chemicals silica gel plates (60F-254) using UV-light (254 and 384 nm), 2.4% phosphomolybdic acid/1.4% phosphoric acid/5% sulfuric acid in water, anisaldehyde in ethanol, or 0.2% ninhydrin in ethanol and heat as developing agents. TSI silica gel (230−400 mesh) was used for flash column chromatography. NMR spectra were recorded on AM300 or AM500 (Bruker) instruments and were calibrated using a solvent peak or tetramethylsilane as an internal reference. The following abbreviations are used to indicate the multiplicities: s, singlet; d, doublet; t, triplet; q, quartet; m, multiplet; br, broad. High-resolution mass spectra were obtained by using EBE geometry.

Compound 1. A solution of *N*-phenylpiperazine (1.82 g, 11.2 mmol) and paraformaldehyde (2.40 g, 79.3 mmol) in MeCN (10 mL) was refluxed for 30 min. Subsequently, 2′,7′-dichlorofluorescein (1.50 g, 3.74 mmol) in 80 mL of H_2O/MeCN (1:1) was added to the resulting solution and the mixture was refluxed for 21 h in the dark. The organic solvent was then removed from the cooled reaction in vacuo. The resulting solution was extracted with CH_2Cl_2 (2 × 200 mL), was dried over Na_2SO_4, and the solvents were evaporated. Silica gel flash chromatography of the residue (2.5→5% MeOH in CH_2Cl_2) was followed by recrystallization in CH_2Cl_2-hexanes to afford compound **1** as a pink solid (2.37 g, 85%). R_f = 0.46 (silica, 5% MeOH in CH_2Cl_2); IR (KBr pellet): ν_{max} = 3431 (br, O−H), 2925, 2814, 1761 (C=O), 1628, 1596, 1495, 1463, 1396, 1284, 1208, 1090, 997, 922, 893, 757, 697 cm^{-1}; ^{1}H NMR (300 MHz, DMSO-d_6, 20 °C): δ = 8.05 (br d, J = 7.2 Hz, 1H), 7.84 (br dd, J = 7.2, 7.2 Hz, 1H), 7.76 (br dd, J = 7.2, 7.2 Hz, 1H), 7.40 (d, J = 7.2 Hz, 1H), 7.20 (br dd, J = 7.2, 7.2 Hz, 4H), 6.93 (br d, J = 7.2 Hz, 4H), 6.78 (t, J = 7.2 Hz, 2H), 6.64 (s, 2H), 4.16 (s, 4H), 3.22 (br s, 4H), 3.13 (m, 4H), 2.89 (br s, 4H), 2.59 (m, 4H); ^{13}C NMR (125 MHz, DMSO-d_6, 20 °C): δ = 151.1, 150.6, 126.5, 124.0, 119.3, 118.8, 115.8, 15.4, 109.1, 21.9, 51, 48.1 (21 expected signals); ES HRMS calcd for $C_{43}H_{43}N_4O_4Cl_2$ $(M + H)^+$: 749.2661; found: 749.2679.

Compound 2. A solution of 4-hydroxy-4-phenylpiperazine (132 mg, 0.747 mmol) and paraformaldehyde (25 mg, 0.798 mmol) in MeCN

(10 mL) was refluxed for 30 min. Subsequently, 2′,7′-dichlorofluorescein (98.2 mg, 0.25 mmol) in 80 mL of H_2O/MeCN (1:1) was added to the resulting solution, and the mixture was refluxed for 21 h in the dark. The organic solvent was then removed from the cooled reaction in vacuo. The resulting solution was extracted with CH_2Cl_2 (2 × 200 mL), was dried over Na_2SO_4, and the solvents were evaporated. Silica gel flash chromatography of the residue (2.5→5% MeOH in CH_2Cl_2) was followed by recrystallization in CH_2Cl_2-hexanes to afford compound **2** in 75% yield as a pink solid. $R_f = 0.22$ (silica, 10% MeOH in CH_2Cl_2); IR (KBr pellet): $\nu_{max} = 3406$ (br, O−H), 1760 (C═O), 1571, 1472, 1370, 1285 cm^{-1}; ^1H NMR (300 MHz, DMSO-d_6, 20 °C): $\delta =$ 8.03 (d, $J = 7.5$ Hz, 1H), 7.8−7.7 (m, 2H), 7.49 (br d, $J = 7.5$ Hz, 4H), 7.35−7.30 (m, 5H), 7.26 (t, $J = 7.5$ Hz, 2H), 6.70 (s, 2H), ∼3.4 (obscured by the solvent), 2.15 (br m, 8H); several ^{13}C NMR experiments resulted in no signals; ES HRMS calcd for $C_{44}H_{41}Cl_2N_2O_7$ $(M + H)^+$: 779.2291; found: 779.2334.

Compound 3. A solution of 1-(4-methoxyphenyl)piperazine (MPP, 1.984 g, 7.48 mmol) and paraformaldehyde (0.747 g, 24.9 mmol) in MeCN (10 mL) was refluxed for 30 min. Subsequently, 2′,7′-dichlorofluorescein (1.50 g, 3.74 mmol) in 80 mL of H_2O/MeCN (1:1) was added to the resulting solution, and the mixture was refluxed for 21 h in the dark. The organic solvent was then removed from the cooled reaction in vacuo. The resulting solution was extracted with CH_2Cl_2 (2 × 200 mL), was dried over Na_2SO_4, and the solvents were evaporated. Silica gel flash chromatography of the residue (2.5→5% MeOH in CH_2Cl_2) was followed by recrystallization in CH_2Cl_2-hexanes to afford compound **3** in 75% yield as a pink solid. $R_f = 0.22$ (silica, 5% MeOH in CH_2Cl_2); IR (KBr pellet): $\nu_{max} = 3434$ (br, O−H), 1765 (C═O), 1512, 1465, 1285, 1248 cm^{-1}; ^1H NMR (300 MHz, DMSO-d_6, 20 °C): $\delta = 8.07$ (d, $J = 7.5$ Hz, 1H), 7.85 (dd, $J = 7.5$, 7.5 Hz, 1H), 7.77 (dd, $J = 7.5$, 7.5, 1H), 7.41 (d, $J = 7.5$ Hz, 1H), 6.99−6.76 (br m, 8H) 6.66 (br s, 2H), 4.18 (br s, 4H), 3.68 (s, 6H), 3.11 (br s, 8H), 2.94 (br s, 8H); several ^{13}C NMR experiments resulted in no signals; ES HRMS calcd for $C_{44}H_{43}Cl_2N_4O_7$ $(M + H)^+$: 809.2509; found: 809.2515.

Compound 4. A solution of 1-(2-pyridinyl)piperazine (1.82 g, 11.2 mmol) and paraformaldehyde (2.40 g, 79.3 mmol) in MeCN (10 mL) was refluxed for 30 min. Subsequently, 2′,7′-dichlorofluorescein (1.50 g, 3.74 mmol) in 80 mL of H_2O/MeCN (1:1) was added to the resulting solution, and the mixture was refluxed for 21 h in the dark. The organic solvent was then removed from the cooled reaction in vacuo. The resulting solution was extracted with CH_2Cl_2 (2 × 200 mL), was dried over Na_2SO_4, and the solvents were evaporated. Silica gel flash chromatography of the residue (2.5→5% MeOH in CH_2Cl_2) was followed by recrystallization in CH_2Cl_2-hexanes to afford compound **4** in 77% yield as a pink solid. $R_f = 0.41$ (silica, 5% MeOH in CH_2Cl_2); IR (KBr pellet): $\nu_{max} = 3435$ (br, O−H), 1764 (C═O), 1594, 1479, 1437, 1400, 1288, 1212, 1094 cm^{-1}; ^1H NMR (300 MHz, CD_2Cl_2, 20 °C): $\delta = 8.15$ (dd, $J = 3.6$, 1.2 Hz, 2H), 8.00 (d, $J = 7.4$ Hz, 1H), 7.76 (ddd, $J = 7.4$, 7.4, 1.2 Hz, 1H), 7.68 (ddd, $J = 7.4$, 7.4, 1.2 Hz, 1H) 7.49 (ddd, $J = 8.5$, 6.9, 1.2 Hz, 2H), 7.21 (br d, $J = 7.4$ Hz, 1H), 6.69−6.62 (m, 6H), 4.12 (d, $J = 14.9$ Hz, 2H), 4.06 (d, $J = 14.9$ Hz, 2H), 3.64 (br s, 8H), 2.81 (br s, 8H); several ^{13}C NMR experiments resulted in no signals; ES HRMS calcd for $C_{40}H_{37}Cl_2N_6O_5$ $(M + H)^+$: 751.2202; found: 751.2233.

MPP Resin. To Aminolink (Pierce) agarose resin (1200 μL, 1 equiv) was added 1-(4-methoxyphenyl)-piperazine (MPP, 47.4 mg, 10 equiv), NaOAc (150 mg, 50 equiv), and $NaBH_3CN$ (27 mg, 43 equiv) in isopropanol (5.1 mL). The mixture was shaken for 2.5 h at 25 °C and then 20 more equiv of $NaBH_3CN$ was added and shaken for 23 additional hours at the same temperature. The resin was then drained and washed with isopropanol (5 mL) and H_2O (10 mL) and was incubated with sat. aq. $NaHCO_3$ (10 mL, 30 min). After washing with H_2O (2 × 12 mL), the white resin was stored in 3 volumes isopropanol at 4 °C. Complete reaction was verified by Schiff's test for free aldehydes (present in unreacted resin).

General Spectroscopic Methods. The cyclodextrins (Aldrich) and 1-(4-methoxyphenyl)piperazine dihydrochloride (Acros Organics) were purchased and used as received. Phosphate buffers (JT Baker) were used after passing through a 22-mm filter.

UV−Vis Spectroscopy. Absorption spectra were acquired on a Cary 50 or a Perkin-Elmer Lambda 19 UV−vis spectrometer, under the control of Windows-based PCs running the manufacturers' supplied software.

Fluorescence Spectroscopy. Fluorescence spectra were acquired in a 1-cm × 1-cm quartz cuvette on a Spex Fluorolog fluorometer under the control of a Windows-based PC running Datamax 32 software. All spectra were corrected for emission intensity using the manufacturer supplied photomultiplier curves.

Quantum Yield Measurements. Quantum yields were determined using fluorescein in 0.1 N NaOH ($\Phi = 0.95$) as a standard. To determine quantum yields relative to fluorescein, stock solutions of compounds **1**−**4** were prepared in DMSO (1 mM) and were diluted in phosphate buffer (pH 7.0, JT Baker) to $OD_{490} = 0.09$. The samples were excited at 490 nm and the integrated emission spectra were compared.

Cyclodextrin Titration. Solutions of **3** (5 μM) in pH 7.4 phosphate buffer (JT Baker) were prepared containing 0−100 mM α-cyclodextrin (by serial dilution of a 100 mM solution of α-cyclodextrin and **3**) or β-cyclodextrin from 0 to 5.0 mM (from a 10 mM β-cyclodextrin stock solution in H_2O). To test the effect of a competitive inhibitor, MPP (3.75 mmol for a final concentration of 2.5 mM) was added to a 5.0 mM β-cyclodextrin solution containing **3**. Samples were excited at 485 nm, and integrated emission spectra were compared using Origin Pro software.

RNA Preparation. DNA templates for the N70 library and biased library and oligonucleotides used for primer extension and RT-PCR were prepared by automated DNA synthesis (Keck Biotechnology Resource Laboratory, Yale University). The random region of the N70 library was synthesized with equimolar concentrations of each base in a 0.2 μmol synthesis. The partially randomized portions of the biased library were prepared by varying the molar proportions of each base during synthesis. Oligonucleotides 40 bases or longer were purified by denaturing (8 M urea) PAGE before use. The N70 pool DNA template (1 nmol) was made double-stranded by extension in the presence of 5′ PR-N70 primer, introducing the promoter for T7 RNA polymerase. DNA extension reactions were carried out using Superscript II Reverse Transcriptase Polymerase (RT, Gibco BRL) according to manufacturer's instructions.

The double-stranded product was then ethanol precipitated, was resuspended in TE buffer, and was transcribed in vitro. Typical transcription reactions (100 μL total volume) included 1 μM template DNA, 40 mM TRIS (pH 7.8), 2.5 mM spermidine, 0.01% Triton X, 2.5 mM each nucleotide triphosphate (ATP, GTP, CTP, UTP), 10 μL T7 polymerase, 10 mM DTT, and 25 mM $MgSO_4$. Each reaction was incubated at 37 °C for 2.5 h. The RNA was then purified via denaturing PAGE, was recovered by elution of excised bands in crush-soak buffer (200 mM NaCl, 10 mM Tris-HCl pH 7.5, 1 mM EDTA pH 8.0), and was ethanol-precipitated.

Preparation of Affinity Media. The MPP Resin or Aminolink (Pierce) agarose resin (120 μL of suspension) was drained of solvent and was washed with selection buffer (8 × 100 μL, 300 mM NaCl, 20 mM Tris-Cl pH 7.4, 5 mM $MgCl_2$).

***In Vitro* RNA Selection.** In typical selection experiments, pool RNA (approximately 10^{13} molecules, ∼900 pmoles) was denatured (100 μL, 300 mM NaCl, 20 mM Tris-Cl pH 7.4, 95 °C, 3 min), was allowed to cool to 25 °C, $MgCl_2$ was added (for a final concentration of 5 mM), and the final mixture was added to the MPP resin (50 μL) and was incubated at 25 °C for 5 min (unless preceded by a negative selection step, in which case the mixture was first incubated on a 50-μL column of unreacted aminolink resin under identical conditions). The column was then washed with selection buffer (8 × 100 μL) and was eluted

with elution buffer (8 × 100 μL). Biased library RNA was subjected to a pre-elution step where the column was washed with elution buffer containing 3 μM MPP prior to elution of binding RNA. RNA from the eluted fractions was pooled and ethanol-precipitated with 50 pmol 5′PR-N70 primer and glycogen (0.1 μg) to be resuspended directly into a 50-μL RT reaction. The resulting cDNA was amplified by PCR (15 cycles) with primers 5′PR-N70 and 3′PR-N70 to generate the template for transcription of RNA for the next round of selection. Typical PCR reactions used the following conditions: 1.5 mM $MgCl_2$, 2.5 μM each primer, 200 μM each dNTP (Roche), and 5 units/100 μL reaction Taq polymerase (Promega) with included buffer. PCR was conducted on an Eppendorf MasterCycler Gradient thermocycler using the following program: 2 min initial denaturation (92.0 °C) followed by 15 cycles of 1 min denaturation (92.0 °C), 1 min annealing (40.8 °C), and 1 min extension (72.0 °C).

Cloning Round 8 cDNA into pCR4-TOPO vector. Round 8 cDNA was then cloned into the pCR4-TOPO vector (Invitrogen) and was used to transform the included chemically competent cells following the manufacturer's supplied protocol. Cultures were grown of 24 colonies (2.5 mL LB-AMP media), and the DNA was isolated using an Eppendorf PerfectPrep Plasmid Mini kit according to the manufacturer's supplied protocol. The plasmid DNA was sent directly to the University of Pittsburgh Molecular Medicine Institute DNA Sequencing Core Facility to be sequenced.

RNA Fluorescence Titrations. RNA aptamers from the N70 Library selection were tested for their ability to enhance the fluorescence of compound **3** by fluorescence titration in 10 × 1 mm quartz cuvettes on a Spex Fluorolog. Emission spectra for **3** were acquired from 500 to 670 nm using an excitation wavelength of 490 nm. Samples were prepared containing 100 μM RNA[66] and 1 μM compound **3** (from a 1 mM DMSO stock solution) in buffer (300 mM NaCl, 20 mM Tris-Cl pH 7.4). The samples were denatured alongside control solutions not containing RNA by heating at 95 °C for 3 min and by allowing to cool to 25 °C. After the addition of $MgCl_2$ (for a final concentration of 5 mM), the solutions were allowed to incubate at 25 °C for 5 min and the fluorescence emission spectra were obtained. Subsequent data points were obtained by dilution. Specifically, 50% of the solution was removed and replaced with an equal volume of compound **3** (1 μM) in selection buffer (300 mM NaCl, 5 mM $MgCl_2$, 20 mM Tris-Cl pH 7.4) effectively halving the RNA concentration (to a minimum of 812 nM) while keeping the chromophore and buffer concentrations constant. Emission spectra were obtained at each data point and the peak intensities at 525 nm were used to construct the titration plot. The control sample not containing RNA falls in line with the nanomolar titration points.

RNA aptamers from the biased library selection were tested using a similar procedure on a Molecular Devices SpectraMax M2 Microplate reader. Excitation was at 490 nm and emission spectra were acquired from 505 to 600 nm. The experimental procedure was similar to the one described above except that the maximum RNA concentration was 50 μM.

MPP Competition Assay. Samples containing **Apt1** RNA (10 μM) and compound **3** (1 μM) in buffer (300 mM NaCl, 20 mM Tris-Cl pH 7.4) were denatured alongside control solutions not containing RNA by heating at 95 °C for 3 min and by allowing to cool to 25 °C. After the addition of $MgCl_2$ (for a final concentration of 5 mM), the solutions were allowed to incubate at 25 °C for 5 min and fluorescence emission spectra were obtained. To determine the effect of MPP on **Apt1** binding, MPP was added (0.1 μL, neat, to a final concentration of 3.2 mM) to each sample.

Acknowledgment. We thank Professors Hiroaki Suga (University at Buffalo), Ronald R. Breaker (Yale University), and Dr. Adam Roth (Yale University) for their help and reviewers for suggesting alternative explanations. This work was supported by the University of Pittsburgh, The Pitt Central Research Development Fund, and the National Science Foundation (CHE-0616577).

JA070111Z

(66) The choice of 100 μM was a practical one, with the yield of each large scale in-vitro transcription reaction yielding only 10−15 nanomoles of RNA.